Journal of Electroceramics, 11, 67–72, 2003
© 2004 Kluwer Academic Publishers. Manufactured in The Netherlands.

Influence of Liquid Phase Additives on Structural and Sintering Behaviour of Samarium Modified Lead Titanate Ceramics

SARABJIT SINGH, O.P. THAKUR & CHANDRA PRAKASH*

Electroceramics Group, Solid State Physics Laboratory, Lucknow Road, Delhi-110054, India

Submitted June 17, 2003; Revised September 13, 2003; Accepted November 18, 2003

Abstract. The combination of metal oxides Bi_2O_3:Li_2O in a ratio 89:11 gives a eutectic with a melting point of ∼680°C. Such a low melting point oxide combination creates a working liquid phase at a highly favorable temperature for use as a densification aid. A liquid—phase sintering aid incorporating Bi_2O_3 and Li_2O is presented which demonstrates not only a reduction in the required sintering temperature but also shows relatively higher 'c/a' ratio (tetragonality) of $PbTiO_3$ ceramics with no fragility of the samples. Detailed dilatometric investigations have been performed in order to study the dominant shrinkage mechanism in the present system. Besides acting as a liquid phase fluxing agent, Bi_2O_3/Li_2O also behave as Curie shifter, which decreases Curie temperature in lead titanate system. The Curie temperature has also been verified from the thermal expansion behavior of sintered specimens. The value of dielectric constant increases after poling which may be due to the dominance of 180° domain wall over 90°.

Keywords: lead titanate, liquid phase, densification, microstructure, dielectric constant

Introduction

Lead Titanate, $PbTiO_3$ ceramics have high Curie temperature (T_c), 490°C and low dielectric constant and these properties make it highly attractive for high-temperature and high frequency applications [1, 2]. However it is very difficult to prepare pure $PbTiO_3$ due to its fragile nature and porous to be polarized [3]. Attempts have been made to produce dense and hard $PbTiO_3$ ceramics by adding additives or by forming solid solution [4, 5]. By substitution of isovalent (Ca^{2+}, Ba^{2+} etc.) or offvalent (Sm^{3+}, Gd^{3+} etc.) ions into the Pb^{2+} sites, the lattice anisotropy is reduced and the samples become denser [6–10]. Another way of improving its mechanical properties is by liquid phase sintering using suitable fluxing agents, Bi_2O_3/Li_2O [11] and PbO [12] had been proven to be promising sintering aids for PMN-PT ceramics. Fluxing agents partly dissolve in lattice and the rest segregates at grain boundary. These additives act as grain growth inhibitors and binders. Addition of Li_2O is most effective for densification while Bi_2O_3 additive gives high resistivity probably by compensating lead vacancies. Since lead titanate ceramics mainly suffer from poor densification and inferior resistivity. Therefore in order to improve these properties we have chosen the eutectic Bi_2O_3:Li_2O (89:11) as liquid phase additive in the present system. The combination of metal oxide, Bi_2O_3:Li_2O in a ratio 89:11 gives a eutectic with a melting point of around 690°C [13]. Such a low melting point creates a working liquid phase at a highly favorable temperature for use as a densification aid.

In the present paper, detailed investigations have been carried out in order to understand the shrinkage mechanism with different concentration of liquid phase and its effect on densification and microstructure.

Experimental Procedure

The compositions investigated were of the type $Pb_{0.98}Sm_{0.02}TiO_3 + x$ wt% (Bi_2O_3/Li_2O = 89/11). Additive concentration x is 0, 0.2, 0.4, 0.6, 0.8, 2, 4

*To whom all correspondence should be addressed. E-mail: prakash@ssplnet.org

and 8 wt%. Excess 2 wt% PbO was taken to compensate the volatilization of PbO during sintering. The starting raw materials were analytical reagent grade of PbO (CDH, India, 99%), Sm_2O_3 (Indian Rare Earth Ltd., India, 99.99%), TiO_2 (CDH, India, 99%), Bi_2O_3 (Aldrich USA, 99.9%) and Li_2CO_3 (Loba Chemie, India, 99%). The weighed components were thoroughly mixed with distilled water in planetary ball mill using zirconia balls as grinding media. The mixtures were dried and then twice calcined at 800°C and 850°C for 4 hrs followed by ball milling. The resulting dried powders were sieved and mixed with PVA organic binder and then pressed at 70 MPa into disc of 10 mm diameter and 1 mm thickness. Pellets were sintered in an upturned alumina crucible where the lid and edge are lapped such that an approximate sealed container is formed. The pressed discs were fired at 1150°C and 1250°C for 4 hrs. A PbO rich atmosphere was maintained with lead zirconate powder to minimize the lead loss during sintering. The suitable firing temperature was determined preliminary from shrinkage of specimens using dilatometer (Orton, Model No. 1600D, USA). Samples up to 2 wt% of additives were almost completely disrupted immediately after cooling or became fragile in a few days. Therefore, in the present paper the results are shown only for 4 and 8 wt% liquid phase additive samples.

Bulk densities of sintered samples were measured using Archimedes principle. Samples were examined by XRD (Philips, PW3020 Diffractometer, Holland) to ensure single-phase formation. For the study of sintering behaviour, green discs of thickness 3 mm were used in dilatometer. Linear thermal expansion studies were carried out on sintered discs and transition temperature were determined. Microstructural study was done using scanning electron microscope (Leo 1430, Japan). For electrical measurements, gold electrodes were sputtered by sputter coater (Denton vacuum LLC, Desk II TSC Cold Sputter/Etch Unit, USA) on major faces of the samples. Dielectric measurements at room temperature were carried out using standard HP 4284A LCR Meter, Japan at 10 kHz on poled and virgin samples. Discs of thickness 0.5 mm were poled at 150°C for 0.5 hr in silicon oil bath with applied dc bias 50 kV/cm.

Results and Discussion

Physical and Dielectric Parameters

Table 1 lists the experimental density of the samples sintered at 1150°C and 1250°C for 4 hrs with different concentration of $(89)Bi_2O_3/(11)Li_2O$ (hereafter referred as 'fluxing agent'). The density increases with increasing concentration of fluxing agent as well as sintering temperature. The maximum density obtained is 7.9 gm/cc (99% of theoretical density) for the sample containing 8 wt% fluxing agent and sintered at 1250°C for 4 hrs. Densification is inhibited at or below 1150°C by the rigid skeleton formed because of contacted points. Once the rigid skeleton is destroyed at higher temperature (1250°C) densification is enhanced [14].

Figure 1 depicts the typical XRD patterns for the samples with 2, 4 and 8 wt% flux agent sintered at 1250°C for 4 hrs. All the samples show single phase with tetragonal structure with major intense peak at (101). Sample with 10 wt% flux agent does not show single phase as some extra lines of Bi_2O_3 and Li_2O appear and hence this particular composition has been ignored for further studies.

The lattice parameters were calculated using standard lattice fit software. Figures 2 and 3 show the variation of lattice parameters ('c' & 'a') and tetragonality (c/a) & unit cell volume respectively with flux concentration of the samples sintered at 1250°C for 4 hrs. Both the tetragonality and cell volume decrease with increase in flux concentration, which may be attributed to

Table 1. Physical and dielectric parameters.

	Sintering temperature							
	1150°C/4 hrs				1250°C/4 hrs			
Composition ($Pb_{0.98}Sm_{0.02}TiO_3$ + x wt% flux agent)	Expt. density (gm/cc)	ε' virgin/ poled	$\tan\delta$(%) virgin/ poled	T_c (°C)	Expt. density (gm/cc)	ε' virgin/ poled	$\tan\delta$(%) virgin/ poled	T_c (°C)
$x = 4$	7.72	180/215	6.5/5	475	7.84	185/190	4/3	465
$x = 8$	7.80	130/210	8/5	471	7.90	135/185	7.5/3	460

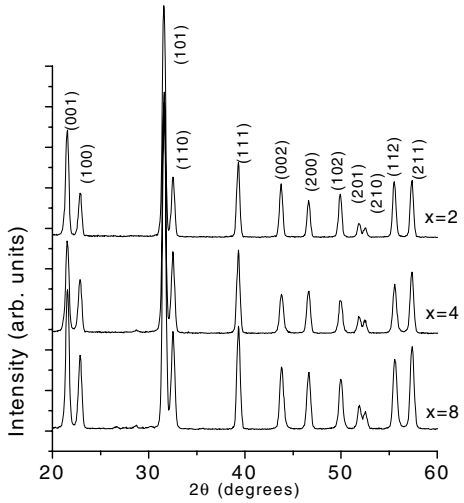

Fig. 1. X-ray diffraction patterns with different concentration of flux agent in the system $Pb_{0.98}Sm_{0.02}TiO_3 + x$ wt% flux agent ($x = 2, 4$ and 8). Samples sintered at 1250°C for 4 hrs.

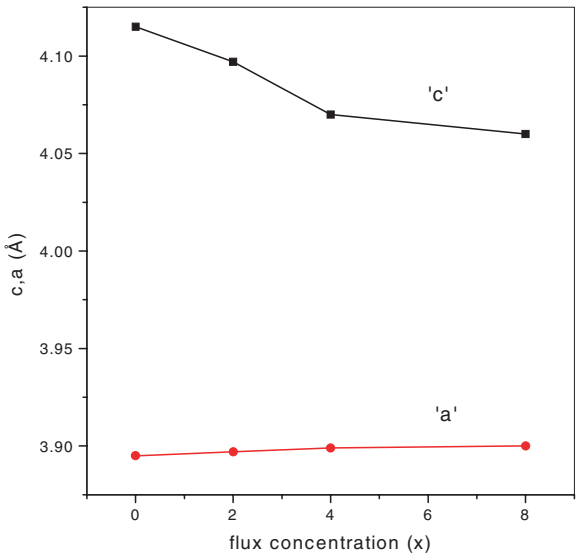

Fig. 2. Variation of lattice parameters ('c', 'a') of the samples sintered at 1250°C for 4 hrs with different concentration of flux agent.

the diffusion of Bi^{3+} ions in the perovskite type tetragonal lattice. However, the tetragonality changed hardly with addition of Li_2O in the composition [15]. The 'c/a' value is higher for the samples sintered at 1150°C as compared to 1250°C. This may be due to a very less rigid skeleton formation at 1250°C avoiding the cracking and reduction in tetragonality.

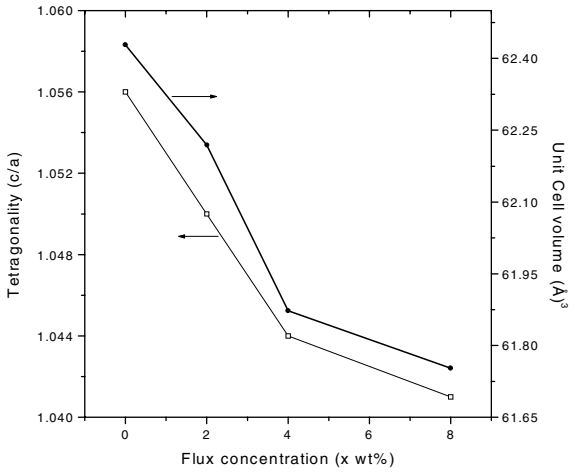

Fig. 3. Variation of tetragonality (c/a) and cell volume of the samples sintered at 1250°C for 4 hrs with different concentration of flux agent.

Figure 4 illustrates the fractured surface micrographs of flux added (4 and 8 wt%) samples sintered at 1150°C and 1250°C for 4 hrs. Micrographs show that as we increase the amount of flux in the composition and increase the sintering temperature, grain size increases a little. Figure 4(a) and (b) shows higher amount of liquid phase and poor crystallinity of the final sintered samples. The porosity is higher for these samples as reflected from black spots. As we increase the sintering temperature, grain develops and micrographs (Fig. 4(c) and (d)) reveal uniform, dense microstructures with spherulitic morphology. Grain size for these samples fall in the range from submicron to approximately 2 μm.

Figure 5 illustrates the typical shrinkage behaviour during sintering of green discs using dilatometer for $Pb_{0.98}Sm_{0.02}TiO_3$ + 4 wt% flux upto 1150°C. Densification of the green sample starts at temperatures above 1050°C. However, some shrinkage is observed at 630°C and indicates a liquid phase locally present, causing liquid rearrangement. This has been further clarified in the Fig. 6 that shows the temperature dependence of shrinkage rate, $d(\Delta L/L_o)/dt$(L_o, initial length of the powder compact; t, time) of the green compacts containing 4 and 8 wt% of fluxing agent. Here, following facts are noteworthy; the shrinkage rates are very high (~0.09) for both the samples. Such a high shrinkage rate cannot be explained in terms of diffusion only. There are nearly three regions for each composition where the shrinkage rate is quite high that

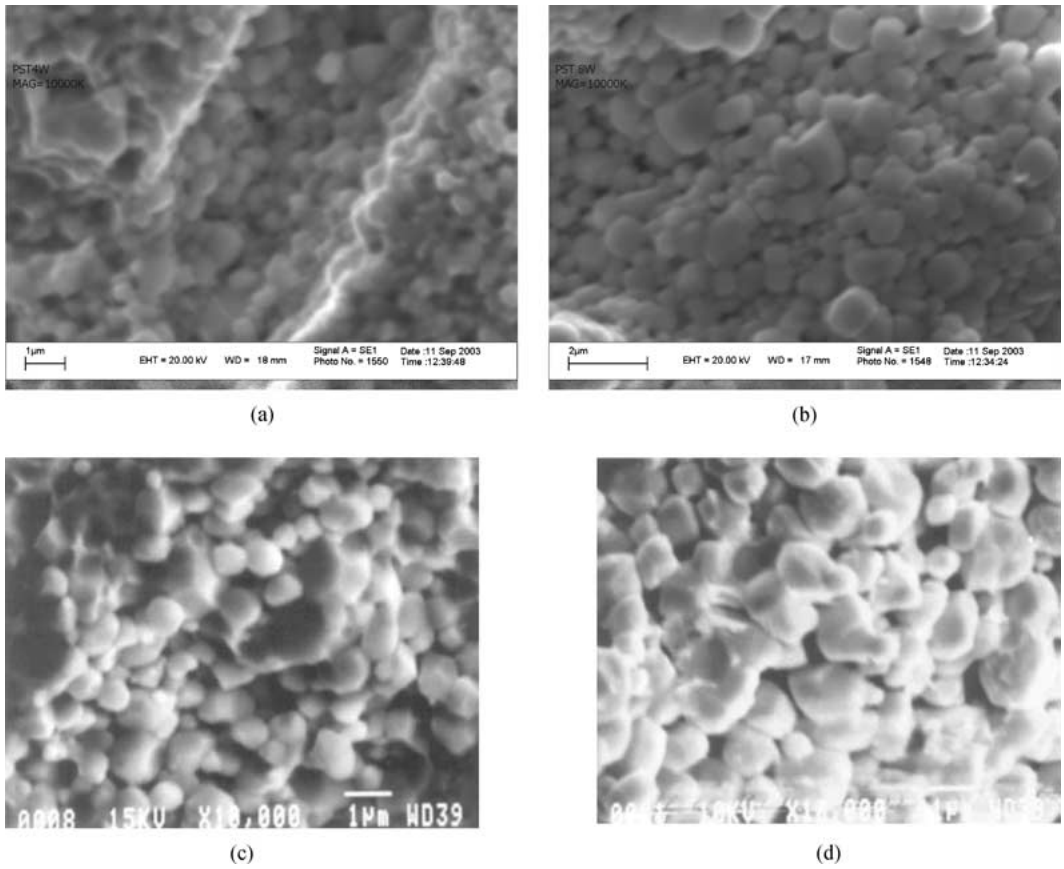

Fig. 4. Scanning electron micrographs for the samples (a) $x = 4$ sintered at 1150°C/4 hrs, (b) $x = 8$ sintered at 1150°C/4 hrs, (c) $x = 4$ sintered at 1250°C/4 hrs and, (d) $x = 8$ sintered at 1250°C/4 hrs of system $Pb_{0.98}Sm_{0.02}TiO_3 + x$ wt% flux agent.

is around 690°C, 850°C & 1150°C for 4 wt% flux agent and 630°C, 790°C and 1060°C for 8 wt% flux agent. The fluxing agent forms the liquid phase around 690°C, so the shrinkage corresponds to the region between 630–690°C is due to the formation of liquid phase. The PbO converts into the liquid phase around 850°C, therefore, second shrinkage region corresponds to the liquid phase formation due to PbO. Finally, some shrinkage occurs around 1150°C that corresponds to the final densification at the sintering temperature. Also one can make out that with the addition of more flux, higher level of densification can be achieved. This observation is in well agreement with the density values as listed in Table 1.

The double logarithmic representation of relative shrinkage vs. dwelling time (Fig. 7) allows the dominating shrinkage mechanism to be verified. Figure 7 clearly indicates that there are two distinct temporal sections in the isothermal shrinkage. In the first period, up to 10 minutes (region AB), the major part of the total isothermal shrinkage occurs. This period is characterized by a slope of unity. The second period from 30 to 100 min (region BC) is specified by the slope of the curve of 0.33–0.5. These different slopes are an indication of different shrinkage mechanisms involved during sintering.

According to the general sintering equation [16]:

$$(\Delta L/L_o)^{m/2} = -(H/2^m R^n)t$$

where, $\Delta L/L_o$ is the relative shrinkage, H is a constant depending on substances and mechanism, R is the radius of the particles, t is time, n is the grain size exponent and m is the shrinkage exponent ($m = 2$, viscous flow; $m = 5$, volume diffusion from the grain boundary; $m = 6$, grain boundary diffusion).

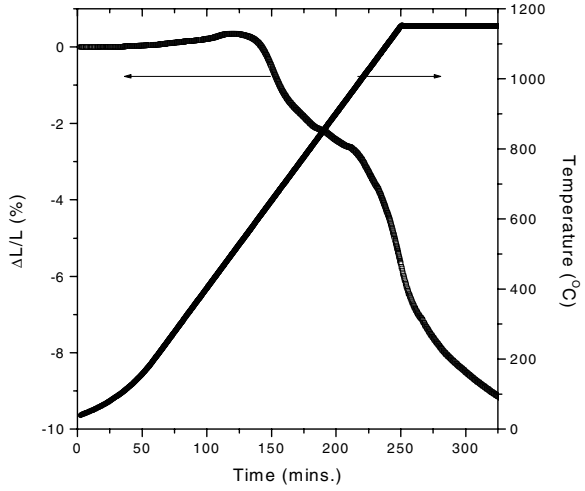

Fig. 5. Typical dilatometric plot for the green sample $Pb_{0.98}Sm_{0.02}TiO_3 + 4$ wt% flux.

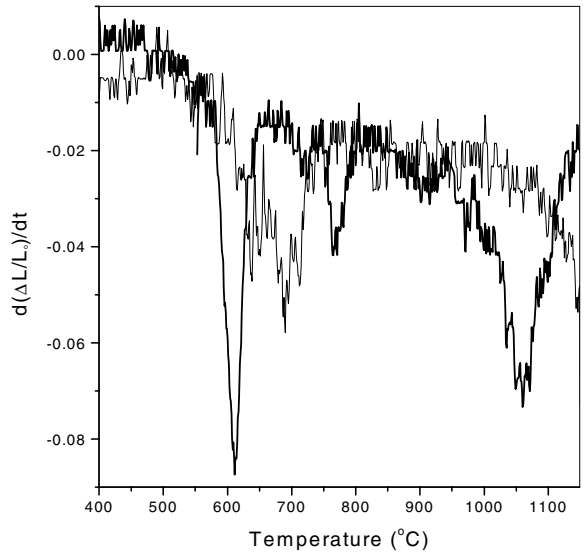

Fig. 6. Temperature dependence of shrinkage rate for the samples $Pb_{0.98}Sm_{0.02}TiO_3 + x$ wt% flux agent ($x = 4$ and 8).

A slope in the isothermal sintering curve of unity ($2/m = 1, m = 2$) corresponds to viscous flow of matter. The slope of the region BC (0.33–0.5) corresponds to the shrinkage exponent $m = 6 - 4$, indicates that grain boundary diffusion and volume diffusion from the grain boundaries are the dominating mechanisms of sintering in this period of isothermal shrinkage. It is also in well agreement with the explanation of liquid

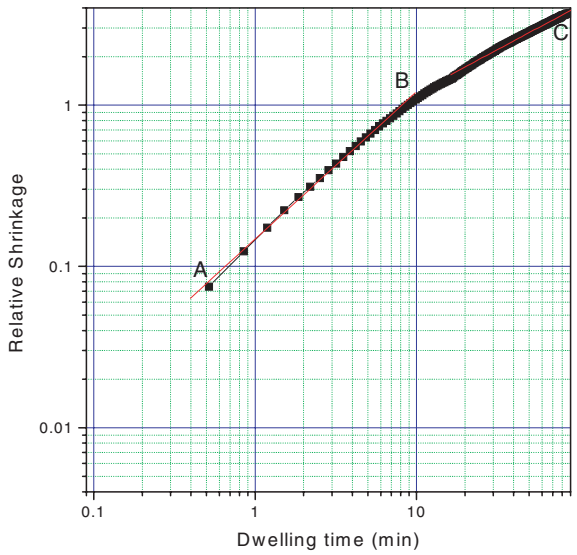

Fig. 7. Typical logarithmic plot of relative shrinkage vs. dwelling time.

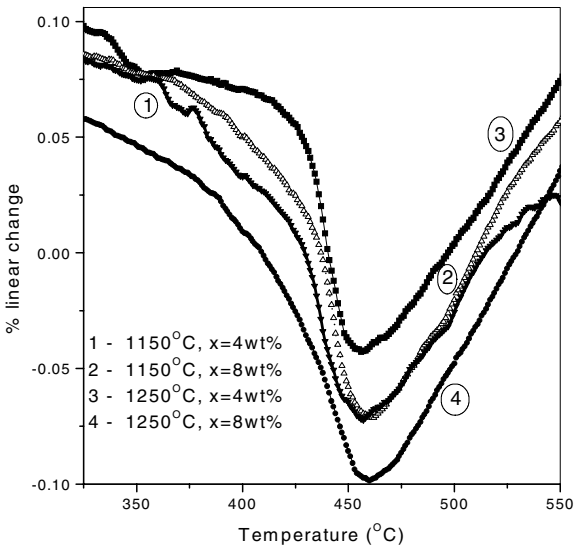

Fig. 8. Thermal expansion behaviour for the discs of composition $Pb_{0.98}Sm_{0.02}TiO_3 + 4$ and 8 wt% flux agent sintered at 1150°C and 1250°C for 4 hrs.

phase sintering behavior due to the addition of flux and due to the presence of PbO.

Figure 8 depicts the thermal expansion behavior of sintered discs for 4 and 8 wt% flux containing compositions sintered at 1150°C and 1250°C for 4 hrs. All these graphs show sudden change in thermal expansion

behaviour near Curie temperature. The drop in thermal expansion occurs due to the structural change of the sample at Curie temperature. The value of Curie temperature obtained from dilatometric plots is in good agreement with the value determined from the temperature dependence plots of dielectric constant (detailed studies to be published elsewhere). The room temperature value of dielectric constant and loss tangent at 10 kHz are listed in Table 1, measured before and after poling. The increase in the value of dielectric constant and decrease in loss as a function of sintering temperature can be explained by the higher crystallinity of perovskite phase and less porosity as seen in SEM photographs. There is increase in density too, which also confirms the reduction in porosity.

It is observed that the value of dielectric constant increases after poling whereas the loss tangent shows opposite trend. The increase in dielectric constant may be due to the dominance of 180° domain rotation over 90° domain, which results in the removal of piezoelectric clamping effect [17], thereby increase dielectric constant.

Conclusions

The X-ray powder diffractometry shows that the present flux agent partly dissolves in the lattice and gives structural change in $PbTiO_3$ lattice. Samples with higher 'c/a' ratio ($\sim$1.058) with good mechanical strength were obtained using flux agent in the present system. From the shrinkage behavior, it is shown that the shrinkage mechanism at first 10 min at particular sintering temperature corresponds to viscous flow of matter while in 30–100 min the shrinkage mechanism is an indicative of grain boundary diffusion and volume diffusion from the grain boundaries. The room temperature value of dielectric constant increases after poling, which is due to the dominance of 180° domain rotation over 90°.

References

1. S. Ikegame, I. Ueda, and T. Nagata, *J. Acoust. Soc. Am.*, **50**, 1060 (1971).
2. T. Takahashi, *Ceram. Bull.*, **69**, 691 (1990).
3. B. Jaffe, R.S. Roth, and S. Marzullo, *J. Res. Nat. Bur. Stand.*, **55**, 239 (1995).
4. E.C. Subbarao, *J. Am. Ceram. Soc.*, **43**, 119 (1960).
5. Y. Matsuo, M. Fujimura, and H. Sasaki, *J. Am. Ceram. Soc.*, **48**, 111 (1965).
6. H. Takeuchi, S. Jyomura, E. Yamamoto, and Y. Ito, *J. Acoust. Soc. Am.*, **72**, 1114 (1982).
7. K. Takeuchi, D. Damjanovie, T.R. Gururaja, S.J. Jang, and L.E. Cross, *Proceedings of the Sixth ISAF* (IEEE, 1986), p. 402.
8. J. Shenglin, Z. Xuli, W. Xiaozhen, and W. Xianghong, *Piezoelect. Acoust.*, **17**, 26 (1995).
9. I. Ueda and S. Ikegame, *Jpn. J. Appl. Phys.*, **7**, 236 (1968).
10. Y. Yamashita, K. Yokoyama, H. Honda, and T. Takahashi, *Jpn. J. Appl. Phys.*, **20**, 183 (1981) .
11. Shen-Li Fu and Gung-Fu Chen, *Proceedings of IMC* (Tokyo, 1998), p. 377.
12. M. Legeune and J.P. Boilot, *Mat. Res. Bull.*, **20**, 493 (1985).
13. E.M. Levin and R.S. Roth, *J. Research Natl. Bur. Standards*, **68A**, 198 (1964).
14. W. D. Kingery, *J. Appl. Phy.*, **30**, 301 (1959).
15. I. Ueda, *Jap. J. Appl. Phys.*, **11**, 450 (1972).
16. D. Voltzke and H.P. Abicht, *Solid State Sciences*, **2**, 149 (2000).
17. M.E. Drougard, *Phys. Rev*., **94**, 1561 (1954).